

## Quantum Mechanical Simulations of Microfracture in a Complex Material

Giulia Galli,<sup>1</sup> François Gygi,<sup>1</sup> and Alessandra Catellani<sup>2</sup>

<sup>1</sup>Lawrence Livermore National Laboratory, Livermore, California 94551

<sup>2</sup>CNR-MASPEC, Via Chiavari, 18/A, I-43001 Parma, Italy

(Received 13 November 1998)

Microfracture in an amorphous semiconductor was investigated by means of first-principles molecular dynamics. A numerical experiment was performed in which a sample of amorphous silicon carbide was subjected to uniaxial strain until failure occurred. The onset of fracture could be unequivocally related to the chemical properties of the constituent species. Rearrangements of atoms following failure indicated a tendency towards Si segregation at the surface. Hardness properties inferred from the stress-strain relationship agree well with experimental data. This type of quantum simulation also provides an unbiased method for generating models of surfaces of complex disordered materials. [S0031-9007(99)09018-3]

PACS numbers: 62.20.Mk, 61.43.Dq, 68.35.Bs, 71.23.Cq

The fracture of materials is a complex phenomenon which requires a multiscale description, involving micro-, meso-, and macroscopic modeling. In the past decades, the classical continuum picture has been used successfully to study materials fracture at the macroscopic level, providing appropriate modeling, except in the region of failure where an atomistic description is required. Recently, meso- and microscopic modelings have been coupled together, using classical simulations and empirical potentials [1,2], which can help elucidate several processes at the atomic level. However, the investigation of fracture in *real materials* calls for models going beyond the continuum picture and atomistic descriptions based on quantum mechanics, thus accounting for bonds breaking in real chemical species.

In this paper we present first-principles computer experiments simulating microfracture in a complex system, and leading to the formation of surfaces. In our calculations, we considered a disordered amorphous semiconductor, composed of two species with different chemical behaviors. Contrary to crystalline solids, where the evolution of dislocations under stress determines the plasticity and eventually the fracture of the material, failure in a disordered solid is expected to be largely determined by the local chemical structure. In particular, we studied amorphous silicon carbide, which is an important material [3] in the technology of photovoltaic devices, solar cells, and hard coatings.

Our results allowed us to relate the onset of failure to the chemical properties of the species constituting the material, and to study the evolution of the electronic structure as the system breaks. In addition, our computer experiment provided an unbiased procedure to generate models of surfaces in an amorphous material. Unlike surfaces of crystals, which are well defined by experimentally known cleavage planes, surfaces of amorphous systems have so far been difficult to characterize, both in experiment and theory. Finally, our computer simulation permitted an *ab initio* determination of elastic as well as hardness properties of a disordered semiconductor.

We first generated a stoichiometric *a*-SiC sample by performing microcanonical *ab initio* molecular dynamics (MD) [4] simulations, and using an annealing-and-quenching technique [5]. We used a 128 atom cell elongated along one of the three Cartesian axes, as shown in Fig. 1a. Total energies, forces, and stress were computed using a plane wave basis set and norm-conserving pseudopotentials. The energy cutoff for the expansion of the single particle orbitals and the charge density are 40 and 160 Ry, respectively. Only Bloch functions at the  $\Gamma$  point of the supercell Brillouin zone were included in the calculations. In our simulations, the initial configuration of the *a*-SiC network was generated by doubling a 64 atom-hydrogenated sample [6], with all hydrogens arbitrarily removed. The system temperature was raised to about 3000 K, thus obtaining a liquid, and then decreased to zero during a 7 ps annealing cycle. In the last part of the annealing cycle the macroscopic density was varied using a damped Andersen dynamics [7] so as to decrease the tensile stress present in the system to less than 2 GPa. The final density was about  $3 \text{ g cm}^{-3}$ . Experimental estimates [8] for samples obtained by chemical vapor deposition (CVD) yield a density of  $2.5 \text{ g cm}^{-3}$ ; however, microvoids are likely to be present, which have not been considered in our calculations. The computer generated *a*-SiC network is well representative of a real material, e.g., a stoichiometric sample grown by CVD [8]: In our system 52% of the bonds are heteronuclear Si-C bonds and 24% are Si-Si bonds, to be compared with the corresponding percentages of 50% and 20% determined experimentally. Theoretically, we find that there are 24% Si dangling bonds, against 20% reported in Ref. [8]. Most importantly we observe a clustering of Si atoms in our calculations, consistent with the presence of Si islands reported for many *a*-SiC samples [8].

In order to investigate how amorphous silicon carbide breaks and forms surfaces, we imposed a tensile strain on the computer generated network, by changing the dimension of one axis of the MD cell ( $z$ ), until fracture

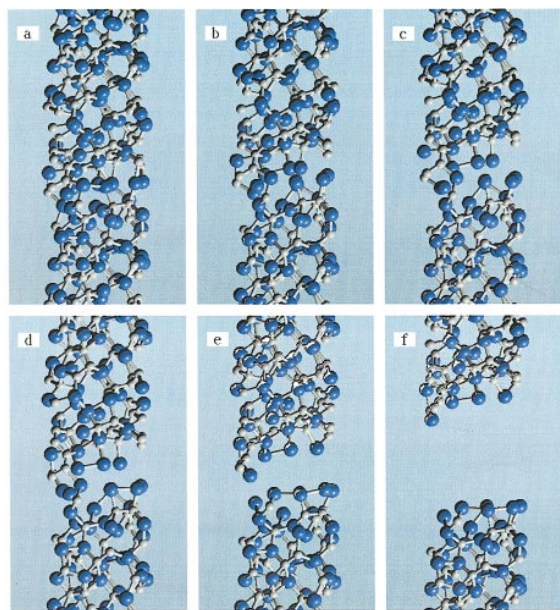


FIG. 1(color). Process leading to the microfracture of the computer generated *a*-SiC network upon elongation along the *z* direction. We considered an MD cell containing 64 Si (blue spheres) and 64 C (grey spheres) atoms, with periodic boundary conditions along *x*, *y*, and *z*. The dimensions of the cell determining the basis set (reference cell) are 16.69, 16.69, and 52 a.u. along *x*, *y*, and *z*, respectively, allowing for a vacuum region of 18.6 a.u., once two surfaces are formed upon fracture. The dimensions of the MD cell before elongation are 16.69, 16.69, and 33.7 a.u. The system before elongation is shown in (a). A microfracture originates in a Si-rich island inside the material (b), proceeds by breaking mostly homopolar Si-Si bonds (c)–(e), and leads to the formation of two surfaces (f). Bonds have been considered as broken when they are longer than the first minimum of the pair-correlation functions of the *a*-SiC network at equilibrium (e.g., before any strain is imposed).

of the system was observed. The strain was applied in 60 discrete steps, after each of which the system was allowed to relax to the closest configuration of minimum energy. In order to ensure a good accuracy in computing energy and forces at each elongation step, we used a plane wave basis set and the same *reference* MD cell throughout the full calculation: The cell was chosen long enough in the *z* direction so as to accommodate two noninteracting surfaces, once the system breaks. The microfracture process and the formation of the two surfaces are illustrated in Fig. 1. The microfracture originates in a Si-rich cluster inside the network: Si-C and Si-Si bonds are first elongated, then rearranged, and eventually broken. The number of heteropolar and homopolar bonds as a function of strain is shown in Fig. 2, where it is seen that the majority of broken bonds upon failure are homopolar Si-Si bonds. Most changes in atomic coordination during elongation occur in the region close to the fracture (within a layer about 2–3 Å thick).

The variation of the total energy and stress during stretching of the material is displayed in Figs. 3 and 4,

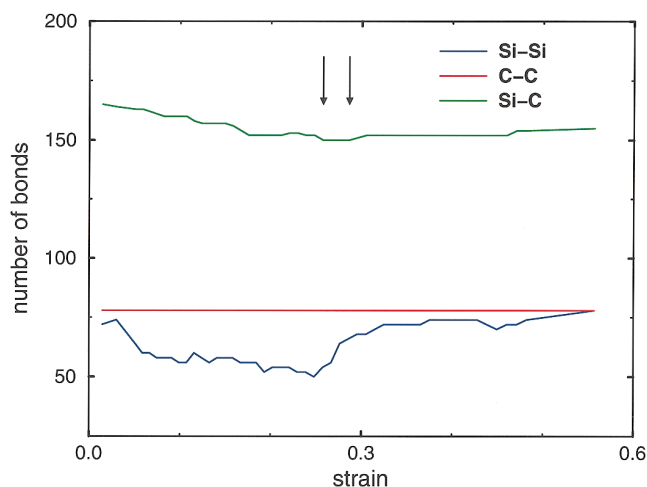


FIG. 2(color). Number of heteropolar and homopolar bonds as a function of strain. The two vertical arrows indicate the values of strain for which the derivative of the total number of bonds is positive and significantly different from zero. The right-hand arrow also corresponds to the value of the strain for which the total energy is maximum (see Fig. 3). After failure, the strain values represent the relative elongation of the MD unit cell.

respectively. Since all of our calculations have been carried out with the same reference cell, the surface formation energy can be estimated as the total energy difference between the initial configuration (bulk) and the configuration after fracture where the surfaces are separated well enough not to interact. We find a small surface formation energy compared to the cubic crystal; indeed in our calculation mostly homopolar Si-Si bonds are broken, which are weaker than the heteropolar Si-C bonds present in the ordered solid. Furthermore, a significant part of the reconstruction energy was gained during bond rearrangements preceding failure. We obtain

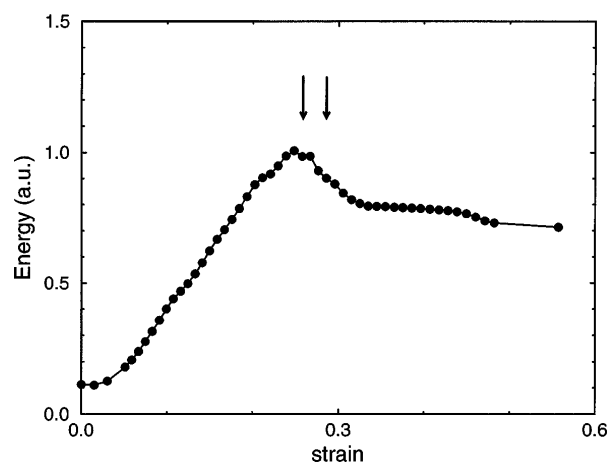


FIG. 3. Total energy as a function of strain. The two vertical arrows indicate the failure region as defined in Fig. 2. After failure, the strain values represent the relative elongation of the MD unit cell.

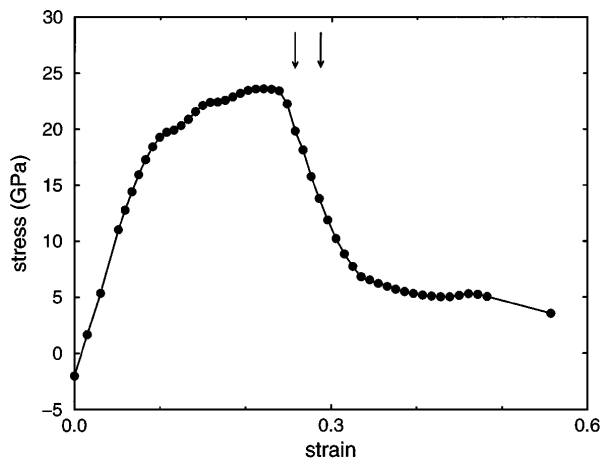


FIG. 4. Stress  $\sigma_{zz} = \frac{\delta \mathcal{E}}{\delta u_{zz}}$  as a function of strain. The maximum value of  $\frac{\delta \mathcal{E}}{\delta u_{zz}}$  before fracture is related to the hardness of the material. The two vertical arrows indicate the failure region as defined in Fig. 2.  $\mathcal{E}$  is the total energy of the system (see Fig. 3).

a value of  $0.2 \text{ eV}/\text{\AA}^2$  for the formation energy of the two surfaces in  $\alpha$ -SiC, to be compared with the values of  $0.32$ – $0.36$  and  $0.58 \text{ eV}/\text{\AA}^2$  for the formation energy of two C- and Si-terminated surfaces, respectively, in  $\beta$ -SiC [9]. We note that a similar observation of a formation energy much smaller than that predicted for crystalline surfaces has been made for surfaces of microscopic hollow defects in cubic SiC [10]. In our calculation, the reconstruction energy (i.e., the energy gained by the surface upon ionic relaxation after fracture) is very small,  $0.035 \text{ eV}/\text{\AA}^2$ , comparable to that computed, e.g., for Si-terminated SiC(001) surfaces of cubic crystalline SiC [9].

The stress as a function of strain (Fig. 4) gives information on both the elastic properties and the hardness of the material. The slope of the stress-strain curve in the linear regime is related to the Young modulus ( $E$ ), whereas the ratio of the maximum load to the surface area in the plastic regime is related to the hardness ( $H$ ) of the material. Our calculated values for  $E$  and  $H$  are 180 and 24 GPa, respectively [11], in good agreement with those measured in nanoindentation experiments [12] (240 and 28–30 GPa).

The two  $\alpha$ -SiC surfaces formed after fracture show considerable roughness even after reconstruction. One surface is solely Si terminated, with mostly 3-fold coordinated Si atoms and a few 4-fold Si atoms. On this surface we observe the formation of several Si dimers (with distances between 2.3 and 2.4  $\text{\AA}$ ) and a microgroove (see Fig. 5). The other surface formed upon fracture contains approximately 60% Si and 40% C atoms, with a short carbon chain close to the surface plane. The C atoms are 2- and 3-fold coordinated, similar to C-terminated reconstructed crystalline surfaces [13]. Interestingly, most in-plane bonds at both surfaces are homopolar bonds.

Given the non-negligible number of dangling bonds at the surfaces, and the presence of a microgroove, we

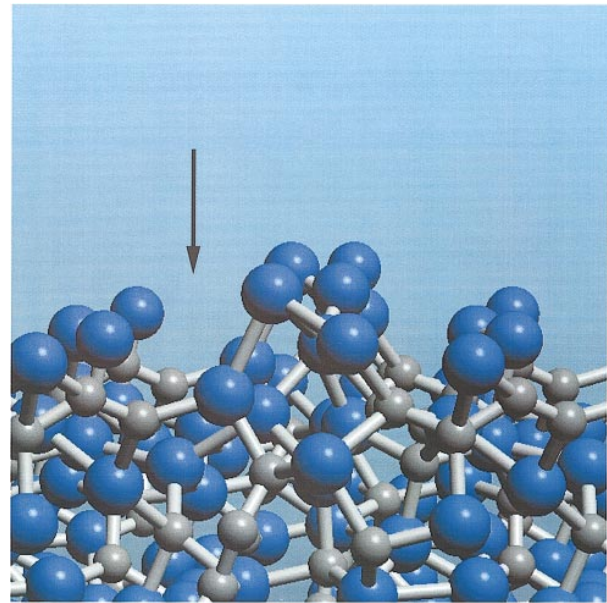


FIG. 5(color). Si-terminated surface formed after fracture (see text). The arrow points to the microgroove. The accumulation of Si atoms at the surface is also visible.

studied the stability of the surface structure as a function of temperature. We carried out two types of computer simulations. We first gave a random displacement to the surface atoms and arbitrarily broke many bonds; we then performed an annealing cycle by heating the whole system to 1000 K and cooling it down again to zero temperature after a short equilibration. This cycle lasted 5 ps. Surprisingly, in both computer experiments, after considerable rearrangement of the atoms at and close to the surface, the system goes back to a configuration energetically and geometrically very close to the starting one. The main changes occur at the surface containing both Si and C atoms, with some C atoms moving inwards, therefore further increasing the Si concentration at the surface. The results of our annealing cycle indicate that the two surfaces formed after fracture correspond to a rather stable atomic geometry and points to the presence of homopolar Si-Si bonds as a genuine characteristic of  $\alpha$ -SiC surfaces. However, the small size of the sample in our simulations and the use of periodic boundary conditions preclude definite conclusions on the presence of microgrooves. The stability of the surface geometry up to about 1000 K is relevant to the use of  $\alpha$ -SiC films as refractory materials.

Besides giving an accurate description of atomic forces, our *ab initio* simulations provide information about electronic structure changes upon elongation of the sample and the electronic properties of the surfaces. In particular, we observed a decrease of 0.8 eV in the valence band width of the computer generated network, before fracture was produced. As soon as failure occurs, the formation of surface states is observed, which lies a few tenths of eV

above the bulk valence band maximum. Surface states are spatially localized on specific sites at the surface, thus giving rise to chemically active Si or C sites. The presence of these active sites can influence the chemical and adhesive properties of specific interfaces, when *a*-SiC is used as a coating material.

In summary, we have presented the first *ab initio* simulations of microfracture in a complex system—an amorphous semiconductor composed of two chemically different species. These calculations open the way to atomistic investigations of fracture and micromechanical properties of complex materials that are not amenable to simulation by classical methods and can be difficult to characterize experimentally. Furthermore, we have presented a way to generate surfaces of an amorphous network, and have shown that first-principles calculations of *both* elastic and hardness properties of disordered materials are feasible and give quantitative agreement with experiment.

Part of this work was performed by the Lawrence Livermore National Laboratory under the auspices of the U.S. Department of Energy, Office of Basic Energy Sciences, Division of Materials Science, Contract No. W-7405-ENG-48. One of us (A.C.) thanks the Lawrence Livermore National Laboratory for its kind hospitality.

- 
- [1] V. Bulatov, F.F. Abraham, L. Kubin, B. Devincere, and S. Yip, *Nature (London)* **391**, 669 (1998).  
 [2] D. Holland and M. Marder, *Phys. Rev. Lett.* **80**, 746 (1998).

- [3] A.W. Nevin, H. Yamagishi, M. Yamaguchi, and Y. Tawada, *Nature (London)* **368**, 529 (1994).  
 [4] R. Car and M. Parrinello, *Phys. Rev. Lett.* **55**, 2471 (1985).  
 [5] F. Finocchi, G. Galli, M. Parrinello, and C.M. Bertoni, *Phys. Rev. Lett.* **68**, 3044 (1992).  
 [6] F. Finocchi and G. Galli, *Phys. Rev. B* **50**, 7393 (1994).  
 [7] See, e.g., *Computer Simulation of Liquids*, edited by M.P. Allen and D.J. Tildesley (Oxford Science, Oxford, 1989), p. 232. In our simulation, the shape of the MD cell was kept orthorhombic.  
 [8] M.A. El Khakani, D. Guay, M. Chaker, and X.H. Feng, *Phys. Rev. B* **51**, 4903 (1995).  
 [9] A. Catellani, G. Galli, F. Gygi, and F. Pellacini, *Phys. Rev. B* **57**, 12 255 (1998).  
 [10] J. Heindl *et al.*, *Phys. Rev. Lett.* **80**, 740 (1998).  
 [11] The Young modulus  $E$  is given by  $E = \frac{\sigma_{zz}}{u_{zz}} \frac{(1+\sigma_p)(1-2\sigma_p)}{(1-\sigma_p)}$ , where  $\sigma_p$  is the Poisson ratio.  $\sigma_p$  enters the definition of  $E$  because in our calculations the stretching was uniaxial, as the  $x$  and  $y$  edges of the MD cell have not been allowed to relax. No attempt has been made to evaluate  $\sigma_p$  and its value (0.22) has been taken from experiment [12]. We note that after surface reconstruction was completed, and the minimization of the total energy of the sample was performed to a great accuracy (atomic forces smaller than  $10^{-4}$  Hartree/Bohr), the residual stress present on the slab could be reduced to 0.3 GPa. This value changed only by a few percent when increasing the kinetic energy cutoff used to define our basis set to 65 Ry.  
 [12] M.A. El Khakani *et al.*, *J. Mater. Res.* **9**, 96 (1994).  
 [13] A. Catellani, G. Galli, and F. Gygi, *Phys. Rev. Lett.* **77**, 5090 (1996).